E. K. Dimitriadis

C. R. Fuller

C. A. Rogers

Smart Materials and Structures Laboratory,
Department of Mechanical Engineering,
Virginia Polytechnic Institute and State University,
Blacksburg, VA 24061

Piezoelectric Actuators for Distributed Vibration Excitation of Thin Plates

The behavior of two dimensional patches of piezoelectric material bonded to the surface of elastic distributed structures and used as vibration actuators is analytically investigated. A static analysis is used to estimate the loads induced by the piezoelectric actuator to the supporting elastic structure. The theory is then applied to develop an approximate dynamic model for the vibration response of a simply supported elastic rectangular plate excited by a piezoelectric patch of variable rectangular geometry. The results demonstrate that modes can be selectively excited and that the geometry of the actuator shape markedly affects the distribution of the response among modes. It thus appears possible to tailor the shape of the actuator to either excite or suppress particular modes leading to improved control behavior.

Introduction

Recent work on novel concepts for both sensing and driving transducers has created strong interest in the active control community. Some of the most significant work has concentrated around the development and implementation of actuators and sensors made of piezoelectric material. The advantage of distributed control as contrasted to point control has been demonstrated by Meirovitch and Norris [1]. Thus, piezoelectric actuators seem to offer a good approach in order to obtain such a control strategy when implemented in patch type configurations.

The feasibility and range of applicability of piezoelectric actuators in one-dimensional vibration excitation and control problems have been demonstrated by a number of researchers [2–4]. In all of these works piezoelements (mostly ceramics) were bonded to the surface of the controlled structure. A rigorous study of the stress-strain-voltage behavior of piezoelectric elements bonded to and imbedded in one dimensional beams was presented by Crawley and de Luis [5]. They analyzed the stresses, strains, and loads generated on a cantilevered beam when piezoelectric segments were bonded symmetrically on both sides. Their work demonstrated a number of important results such as increased effectiveness of the actuators for stiffer and thinner bonding layers, as well as for stiffer piezoelectric material. Another important observation of Crawley and de Luis is that the effective moments resulting from the piezoactuators can be seen as concentrated on the two ends of the actuator when the bonding layer is assumed infinitely thin.

Bailey and Hubbard [6] recently developed and implemented three different control algorithms on a beam piezoelectric system to control transient cantilevered beam vibration. Part of this work involved developing equations for the response of a cantilevered beam with a layer of polyvinylidene fluoride (PVF_2) bonded to one complete side of the beam. The algorithms were experimentally tested and simultaneous control of the first three modes was demonstrated.

Other workers who have performed significant research on the use of the piezoelectric actuators are Fanson and Chen [7] and Baz and Poh [8]. These works, on control of motion in beams, again have demonstrated the potential of piezoelectrics as distributed vibration actuators by simultaneously controlling a number of modes with reduced spillover.

Although these previous works have clearly shown the tremendous potential of piezoelectric actuators, the investigations have been limited to actuation of one dimensional systems such as beams. Of course, many systems are composed of distributed two dimensional elements such as panels and there is need to understand whether piezoelectric actuators can successfully control motion in such systems. The present paper thus deals with an approximate analytical investigation of the actuation of two dimensional thin elastic structures by piezoelectric patches symmetrically bonded to the opposite plate surfaces.

The current work is thus an extension of the one dimensional theory derived by Crawley and de Luis [5]. Piezoelectric elements which are finite in two dimensions are considered. The potential of two dimensional patches is investigated through static and dynamic analyses. The static analysis estimates the loads induced by the piezoelectric actuator to the supporting thin elastic structure. This is followed by an approximate dynamic analysis model for an undamped thin rectangular plate with simply supported boundary conditions excited by a rectangular piezoelectric patch of variable dimensions. Results are presented for the vibration displacement distribution and modal amplitudes of the panel response for various excitation frequencies and actuator dimensions. The effectiveness of the patch actuator in generating a single mode with reduced excitation of other unwanted modes (spillover) is briefly investigated.

Contributed by the Technical Committee on Vibration and Sound for publication in the JOURNAL OF VIBRATION AND ACOUSTICS. Manuscript received December 1989; revised June 1990.

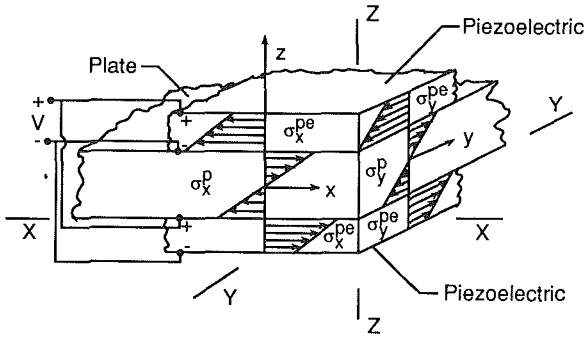

Fig. 1 Stress distribution, *x-z* and *y-z* planes, due to piezoelectric activation

Actuator Analysis

Piezoelectric elements or "patches," when unconstrained and activated by applying a voltage along their polarization direction develop compressive (or extensional depending upon the input voltage sign) strains. In an unconstrained two-dimensional actuator, which is polarized in the z-direction, equal strains will be induced in both the x and y-directions when activated. The magnitude of the induced strains can be expressed as a function of the piezoelectric-strain constant, d_{31}, the applied voltage, V, and the actuator thickness, t:

$$(\epsilon_x)_{pe} = (\epsilon_y)_{pe} = \epsilon_{pe} = \frac{d_{31}}{t} V \tag{1}$$

The subscripts pe and p denote quantities associated with the piezoelectric elements and the plate, respectively.

In the following model formulation and simulation, the piezoelectric elements are assumed to be perfectly bonded to the surface of an infinite plate. In order to maintain symmetry of the geometric structure and increase the authority of the actuator patches, a piezoelectric patch is bonded on both the top and bottom surface of the plate. The two actuators are then activated by applying a voltage of opposite signs to the opposing piezoelectric patches. The uniform surface tractions caused at the actuator-plate interfaces, act in opposite directions and being off the neutral axis they cause uniform bending-moments as a reaction to the actuator. These bending moments are uniform within the actuator boundaries, which for the time being is assumed to be of infinite extent. If so, the symmetry of the elements on the top and bottom surfaces result in no net extension or contraction of the plate midplane. The plate then deforms in pure bending.

The assumption of perfect bonding between the actuator patch and the plate implies that strain continuity is specified at the interface. With the interface strains of the plate and the piezoelectric element being equal and the elastic moduli of the materials being different the interface stresses will contain a discontinuity. This discontinuity will also be created by the additional "external" stress caused by activating the piezoelectric element. The general form of the stress distribution is shown in Fig. 1 [5, 6]. Because the actuators strain normal to their polarization direction, the induced interface stresses and strains are equal in the x- and y-directions and the resulting stress distributions in the x-z y-z planes are identical at all points constrained by the piezoelectric elements. Therefore, Fig. 1 represents the x-z and y-z stress distribution at any point within the piezoelectric-plate structure.

Before proceeding further in developing the piezoelectric actuator induced stress relations, it is appropriate to consider the nature of the plate deformation resulting from activation of surface bonded distributed actuators. From Fig. 1 it is clearly shown that, at any point within the actuator patch boundary, the stress distribution within the plate must be symmetric about the neutral axis (as no extension is possible from equilibrium considerations) and bending of the plate yields a linear normal stress distribution. The actuator stresses can be integrated to obtain the equivalent bending moment. Once the interface stress of the plate is found (or the equivalent bending stress at the plate surface) the resulting plate bending response can be found.

For instance, the normal stress distribution, as shown in Fig. 1, within the plate can be reduced to couples per unit length by

$$\int_{-h}^{h} \sigma_x z \, dy \, dz = m_x dy$$
$$\int_{-h}^{h} \sigma_y z \, dx \, dz = m_y dx \tag{2}$$

The strain distribution through-the-thickness is linear and can be determined from

$$\epsilon_x = \frac{z}{r_x}; \ \epsilon_y = \frac{z}{r_y} \tag{3}$$

where $1/r_x$ and $1/r_y$ denote the curvatures of the neutral surface parallel to the x-z and y-z planes at any point on the plate. When equations (3) are substituted into Hooke's Law and equations (2) used to replace the normal stresses, σ_x and σ_y, with the couples, m_x and m_y, the following expressions are obtained [9]

Nomenclature

- A = area of plate
- C_0 = piezoelectric strain-plate moment coupling term
- d_{31} = piezoelectric strain constant
- D = flexural rigidity
- E = Young's modulus
- h = half-thickness of plate
- $h(\bullet)$ = step function
- K = geometric nondimensional parameter
- L = plate dimension
- m = interface moments per unit length
- m'' = mass per unit plate area
- M = internal plate moments
- P = constitutive nondimensional parameter
- r = radius of curvature
- t = piezoelectric element thickness
- V = voltage
- w = plate transverse displacement
- W = plate amplitude of displacement
- x,y,z = rectangular coordinates (centered on the plate neutral axis)
- x_1,x_2, y_1,y_2 actuator boundaries

Greek

- γ = plate wavenumber
- $\delta(\bullet)$ = delta function
- ϵ = strain
- ν = Poisson's ratio
- σ = stress
- ϕ_{mn} = plate eigenfunction
- ω = input frequency
- ω_{mn} = resonance frequency

Subscripts

- i = interface between actuator and plate
- p = plate
- pe = piezoelectric element
- m,n = modal indices
- x = x-direction
- y = y-direction

$$m_x = D\left(\frac{1}{r_x} + \nu\frac{1}{r_y}\right)$$

$$m_y = D\left(\frac{1}{r_y} + \nu\frac{1}{r_x}\right) \tag{4}$$

where D is the flexural rigidity of the plate, $\frac{Eh^3}{3(1-\nu^2)}$. For any rectangular piezoelectric element, the unconstrained strains in the x- and y-directions are equal which will result in the couples m_x and m_y to be equal and uniformly distributed over the entire plate within the actuator boundaries. It can now be easily seen that in order to satisfy equations (4) r_x must equal r_y at all points within the piezoelectric patch which is the definition of pure plate bending. In fact, this conclusion can be confirmed for a plate of any shape in which the bending moments are uniformly distributed along the entire boundary (or uniformly distributed throughout the plate) and no twistive moments exist, resulting in a plate bent to a spherical surface of curvature given by

$$\frac{1}{r_x} = \frac{1}{r_y} = \frac{m}{D(1+\nu)} \tag{5}$$

Based on this result, the objective will be to determine the magnitude of the edge moments to be applied to the plate in order to replace the actuator patch and create pure bending of the plate such that the bending stress at the surface of the plate is equal to the plate's interface stress when the patch is activated.

This formulation begins with determining the plate and piezoelectric patch interface stress-strain relations derived directly from Hooke's Law

$$(\sigma_{x_i})_p = \frac{E_p}{1-\nu_p^2}(\epsilon_{x_i} + \nu_p\epsilon_{y_i})$$

and

$$(\sigma_{y_i})_p = \frac{E_p}{1-\nu_p^2}(\epsilon_{y_i} + \nu_p\epsilon_{x_i}) \tag{6}$$

The actuator stresses at the interface is the result of superimposing the external plate strains at the interface and the unconstrained piezoelectric element strains

$$\begin{aligned}(\sigma_{x_i})_{pe} &= \frac{E_{pe}}{1-\nu_{pe}^2}[\epsilon_{x_i} + \nu_{pe}\epsilon_{y_i} - \epsilon_{pe} - \nu_{pe}\epsilon_{pe}] \\ &= \frac{E_{pe}}{1-\nu_{pe}^2}[\epsilon_{x_i} + \nu_{pe}\epsilon_{y_i} - (1+\nu_{pe})\epsilon_{pe}] \\ (\sigma_{y_i})_{pe} &= \frac{E_{pe}}{1-\nu_{pe}^2}[\epsilon_{y_i} + \nu_{pe}\epsilon_{x_i} - (1+\nu_{pe})\epsilon_{pe}]\end{aligned} \tag{7}$$

The bending stresses in the plate are linear in z and can be written in terms of their values at the interface as,

$$(\sigma_x)_p = \frac{(\sigma_{x_i})_p}{h}z;\ (\sigma_y)_p = \frac{(\sigma_{y_i})_p}{h}z \tag{8}$$

Similarly, the stress distribution in the piezoelectric element is assumed to have the same slope as in the beam and is

$$(\sigma_x)_{pe} = (\sigma_{x_i})_{pe} - (\sigma_{x_i})_p\left[1 - \frac{z}{h}\right] \tag{9}$$

while a similar equation in the y-direction can be written. Since we have established that pure bending is an appropriate assumption, only the x-direction equations will be presented with the understanding that in all cases there is a companion y-direction equation.

Once the interface stress of the plate is known from equation (6), the uniformly distributed moments can be determined to produce the assumed linear stress distribution. However, equations (6) are functions of the unconstrained piezoelectric strain, ϵ_{pe}, and the actuator interface strains. Therefore, the interface strains and the plate bending stresses must be derived in terms of the constituent material properties and the unconstrained actuator strains. The relationship between $(\sigma_{x_i})_p$ and $(\sigma_{x_i})_{pe}$ is determined from moment equilibrium about the neutral axis of the plate.

$$\int_0^h (\sigma_x)_p z\,dz + \int_h^{h+t} (\sigma_x)_{pe} z\,dz = 0 \tag{10}$$

Equations (8) and (9) are substituted into equation (10) to evaluate the integral, resulting in

$$(\sigma_{x_i})_p = \frac{3th(2h+t)}{2(h^3+t^3)+3ht^2}(\sigma_{x_i})_{pe} \tag{11}$$

or

$$(\sigma_{x_i})_p = K(\sigma_{x_i})_{pe} \tag{12}$$

where the nondimensional geometric parameter, K, is defined as

$$K = \frac{3th(2h+t)}{2(h^3+t^3)+3ht^2} \tag{13}$$

In a similar fashion, the interface stress relations are developed in the y-direction. Equation (12) may now be substituted into equations (6) and (7) in order to eliminate the interface plate strains from the expressions

$$(1-P)\epsilon_{x_i} + (\nu_p - P\nu_{pe})\epsilon_{y_i} = -(1+\nu_{pe})P\epsilon_{pe} \tag{14}$$

where

$$P = -\frac{E_{pe}}{E_p}\frac{1-\nu_p^2}{1-\nu_{pe}^2}K \tag{15}$$

The interface strain relation can be determined by simply rearranging equation (14)

$$\epsilon_{x_i} = \epsilon_{y_i} = \frac{-(1+\nu_{pe})P}{1+\nu_p-(1+\nu_{pe})P}\epsilon_{pe} \tag{16}$$

Now that the interface strains have been reduced to a function of the unconstrained piezoelectric element strains and the constitutent material properties, the uniformly distributed moments which produce the interface stress, $(\sigma_{x_i})_p$, can be determined. Substituting the bending curvature-stress relationship [9] into equation (4) results in the expression

$$m_x = m_y = \frac{2}{3}h^2(\sigma_{x_i})_p \tag{17}$$

When the interface stress-piezoelectric strain coupling relations, equations (6) and (16), are substituted into equation (17) the distributed surface moments may be expressed as

$$m_x = m_y = C_0\epsilon_{pe} \tag{18}$$

where

$$C_0 = -E_p\frac{1+\nu_{pe}}{1-\nu_p}\frac{P}{1+\nu_p-(1+\nu_{pe})P}\frac{2}{3}h^2 \tag{19}$$

The formulation above began with several basic assumptions of which the first was that the plate and patch are considered infinite. Naturally, the piezoelectric patches are finite thereby necessitating a brief discussion on the appropriateness of the above formulation. For a finite actuator patch, the normal

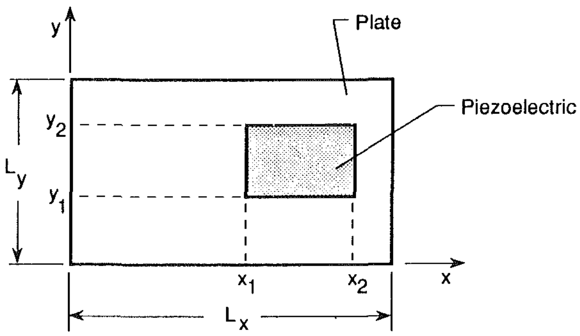

Fig. 2 Plate and piezoelectric actuator coordinate system

stress distribution as shown in Fig. 1 does not hold at the free-edge where equilibrium conditions require the normal stress at the actuator boundary to be zero. However, Liang and Rogers [10] showed that the actuator stress field for a distributed actuator is unaffected by the free-edge up to approximately four actuator thicknesses from the boundary. Therefore, for large actuators with respect to their thickness, the assumed stress field described above and shown in Fig. 1 creates a case of pure plate bending which is the fundamental working premise of the formulation. Crawley and de Luis [5] have also shown that when a finite piezoelectric strip is "perfectly" bonded to a beam, the induced moments effectively act at the element boundaries and result in pure bending of a one-dimensional structure. It will be shown in the following derivation of the excitation of a plate by a finite piezoceramic patch that this concept can be extended to two dimensions; the induced moments can be effectively thought of as acting at the piezoceramic element boundaries. These moments will be constant per unit length in both the x and y directions.

Excitation of a Simply Supported Rectangular Plate

We now turn to the vibration model of a finite plate with a bonded rectangular actuator as viewed from the top in Fig. 2. The plate in the ensuing analysis will be assumed rectangular with simply supported boundaries. As required by the previous analysis the actuator is taken to consist of two identical piezoceramic elements bonded symmetrically to each side of the plate so that their edges are parallel to the plate edges.

The activated piezoelectric actuator will induce internal moments across the piezoelectric and since, as previously shown, the strains are the same in the two directions, these moments are independent of the actuator length. The moments in the plate can be written using unit step functions

$$m_x = m_y = C_0\epsilon_{pe}[h(x-x_1) - h(x-x_2)][h(y-y_1) - h(y-y_2)] \quad (20)$$

Here, $h(\cdot)$ is the unit step function.

If the actuator input voltage is oscillating, moments m_x and m_y will oscillate at the same frequency as the voltage. It is now possible to write the equation of motion for the plate. It is assumed at this point that the mass and stiffness loading of the plate by the bonded actuator are negligible. Using classical thin plate theory, the equation of motion can be written in terms of the internal plate bending moments, M_x, M_y, and M_{xy}, and the actuator induced moments, m_x and m_y, as

$$\frac{\partial^2(M_x - m_x)}{\partial x^2} + 2\frac{\partial^2 M_{xy}}{\partial x \partial y} + \frac{\partial^2(M_y - m_y)}{\partial y^2} + m''\ddot{w} = 0 \quad (21)$$

m'' being the area mass density of the plate, and w the plate transverse displacement [9].

The moments, m_x and m_y, can be transferred to the right hand side of equation (21), thus representing the external plate loads. In addition, the internal moments, M_x, M_y, and M_{xy}, can be written in terms of the displacement w [9], yielding the final equation of motion

$$D\nabla^4 w + m''\ddot{w} = \frac{\partial^2 m_x}{\partial x^2} + \frac{\partial^2 m_y}{\partial y^2} \quad (22)$$

where D is the plate flexural rigidity.

The external loads in equation (22) can be calculated by differentiating equation (20).

$$\frac{\partial^2 m_x}{\partial x^2} = C_0\epsilon_{pe}[\delta'(x-x_1) - \delta'(x-x_2)][h(y-y_1) - h(y-y_2)] \quad (23)$$

and

$$\frac{\partial^2 m_y}{\partial y^2} = C_0\epsilon_{pe}[h(x-x_1) - h(x-x_2)][\delta'(y-y_1) - \delta'(y-y_2)] \quad (24)$$

When the above expressions are substituted into equation (22), the equation of motion becomes

$$D\nabla^4 w + m''\ddot{w} = C_0\epsilon_{pe}[\delta'(x-x_1) - \delta'(x-x_2)][h(y-y_1) - h(y-y_2)] + C_0\epsilon_{pe}[h(x-x_1) - h(x-x_2)][\delta'(y-y_1) - \delta'(y-y_2)] \quad (25)$$

It is easy to show that a moment, M, acting upon a structure can be represented by a dipole force whose magnitude is $M\delta'(x-x_0)$, where x_0 is the location of the moment. Loads of the same nature (here, line moments), appear as the resultant plate excitation in equation (25). It can thus be said that the uniformly distributed reaction moments in the plate are the result of external line moments acting along the boundaries of the piezoelectric element.

The solution of equation (25) can be reached using the modal expansion of the response $w(x,y)$. For a simply supported rectangular plate the eigenfunctions are,

$$\phi_{mn}(x,y) = \sin(\gamma_m x)\sin(\gamma_n y) \quad (26)$$

where $\gamma_m = m\pi/L_x$ and $\gamma_n = n\pi/L_y$.

The plate response to the piezoelectric actuator may now be expanded in terms of the above eigenfunctions, while the harmonic term has been suppressed for brevity

$$w(x,y) = \sum_{m=1}^{\infty}\sum_{n=1}^{\infty} W_{mn}\phi_{mn}(x,y) \quad (27)$$

Here, W_{mn} are plate response modal amplitudes which can be calculated by substituting $w(x,y)$ from equation (27) back into the equation of motion

$$\sum_{m,n}(\omega_{mn}^2 - \omega^2)W_{mn}\phi_{mn}(x,y) = \frac{1}{m''}\left[\frac{\partial^2 m_x}{\partial x^2} + \frac{\partial^2 m_y}{\partial y^2}\right] \quad (28)$$

Mode orthogonality can now be implemented in equation (28), resulting in the expression for the modal amplitudes, W_{mn},

$$W_{mn} = \frac{4C_0\epsilon_{pe}}{m''A(\omega_{mn}^2 - \omega^2)}\left[-\frac{\gamma_m^2 + \gamma_n^2}{\gamma_m\gamma_n}(\cos\gamma_m x_1 - \cos\gamma_m x_2)(\cos\gamma_n y_1 - \cos\gamma_n y_2)\right] \quad (29)$$

It is worthwhile to summarize the important approximations used in the preceding analysis. It is assumed that the piezoelectric element is perfectly bonded to the plate thus the interface strains in the actuator and plate are equal. As discussed by Crawley and de Luis [5], significant thickness of adhesive can affect this situation. The piezoelectric element is also assumed to not significantly alter the inertial mass or effective stiffness of the plate. This assumption of course is dependent upon the relative size, weight, and stiffness of the actuator but

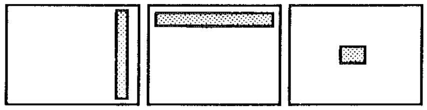

Fig. 3 Piezoelectric actuator test configuration

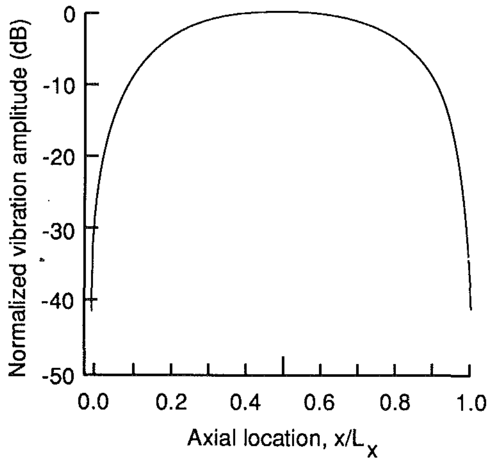

Fig. 4 Displacement distribution, configuration I, $\omega = 430$ rad/sec

Table 1 Material properties

$E_p(\times 10^9\ N/m^2)$	$\rho(kg/m^3)$	ν	C_L^S (m/sec)
207	7870	0.292	3096 (shear)

Table 2 Plate resonant frequencies, ω_{mn}(rad/sec)

m \ n	1	2	3	4	5	6
1	437.5	1246.0	2593.5	4480.0	6905.5	9870.0
2	941.4	1749.9	3097.4	4983.9	7409.4	10373.9
3	1781.2	2589.7	3937.2	5823.7	8249.2	11213.7
4	2957.0	3765.5	5113.0	6999.5	9425.0	12389.5
5	4468.8	5277.3	6624.8	8511.3	10936.7	13901.2

is likely to be reasonably accurate for small actuators such as piezoceramics commercially available with thicknesses of the order of 0.2 mm. This will be studied experimentally in the near future.

Results

Example results are presented for the excitation of a rectangular thin elastic plate excited by a pair of rectangular piezoelectric patches (an actuator) of various dimensions. The plate was assumed to be steel with material properties given in Table 1. The dimensions of the plate were; $L_x = 0.38$ m, $L_y = 0.30$ m, and half-thickness $h = 0.7938$ mm. Resonant frequencies for modes (m,n) were calculated from thin plate theory [11] and are given in Table 2.

For the following results no attempt was made to optimize the actuator shape or location to selectively excite modes; this is the subject of ongoing research. Rather the work presented here is intended to be preliminary in nature in order to demonstrate that it is possible to excite two dimensional modes with patch type piezoelectric actuators.

Three different configurations of actuators were tested and their layout is given in Fig. 3. For the first four results, the shape of the piezoelectric actuator was held constant as in configuration I at $x_1 = 0.32$ m, $x_2 = 0.36$ m, $y_1 = 0.04$ m, $y_2 = 0.26$ m; this is a long and narrow element along the y-direction and symmetric about the $L_y/2$ line. The input frequency is varied. For the second case of configuration II, the input frequencies are kept constant and the location of the actuator varied. In the last case of configuration III a small actuator is placed at the center of the plate. All the plate vibration profiles were calculated along the $y = L_y/2$ line and are presented normalized to the maximum obtained value.

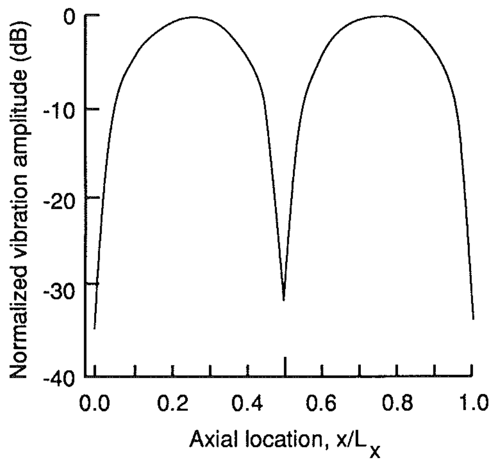

Fig. 5 Displacement distribution, configuration I, $\omega = 930$ rad/sec

Table 3 Plate displacement amplitudes (dB), $\omega = 430$ rad/sec)

m \ n	1	2	3	4	5	6
1	0.0	-652.5	-63.6	-668.8	-72.6	-666.8
2	-28.6	-650.6	-59.8	-664.4	-67.8	-661.9
3	-33.2	-651.8	-59.5	-663.3	-66.2	-660.0
4	-37.1	-654.3	-60.9	-664.0	-66.5	-660.1
5	-45.0	-661.1	-66.5	-668.6	-70.4	-663.3

Table 4 Plate displacement amplitudes (dB), $\omega = 930$ rad/sec)

m \ n	1	2	3	4	5	6
1	-42.1	-648.3	-64.4	-670.3	-74.2	-668.5
2	0.0	-650.0	-60.9	-665.9	-69.4	-663.6
3	-32.7	-652.6	-60.8	-664.8	-67.9	-661.8
4	-38.1	-655.6	-62.4	-665.6	-68.2	-661.8
5	-46.6	-622.8	-68.2	-670.3	-72.1	-665.1

Excitation Frequency $\omega = 430.00$ rad/sec. Figure 4 shows the total plate displacement amplitude for input excitation frequency of $\omega = 430.00$ rad/sec and configuration I. As can be seen from Table 2, this frequency is close to the resonant frequency of the (1,1) mode and it is apparent from Fig. 4 that this mode is being strongly excited with the response plot close to that for a (1,1) mode shape. Likewise the normalized modal amplitudes presented in Table 3 for this case show that the (1,1) is indeed strongly excited being close to 30 dB up on the next mode. From the results of Table 3 it also appears that spillover of energy is occurring among the next higher order modes with nodal lines parallel to the long side of the actuator or the y axis. Modes with nodal lines perpendicular to the actuator are not excited at all. This is to be expected since the line moments are all in phase along the y direction.

Excitation Frequency $\omega = 930.00$ rad/sec. Figure 5 and Table 4 present similar results when the input frequency is $\omega = 930.00$ rad/sec or close to the resonant frequency of the (2,1) mode. The displacement amplitude distribution in Fig. 5 shows evidence of the (2,1) mode being dominant with very

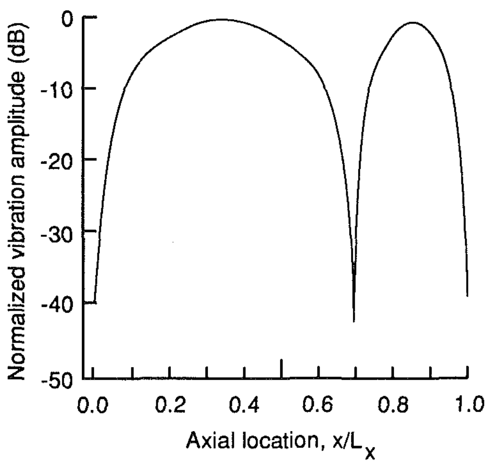

Fig. 6 Displacement distribution, configuration I, $\omega = 600$ rad/sec

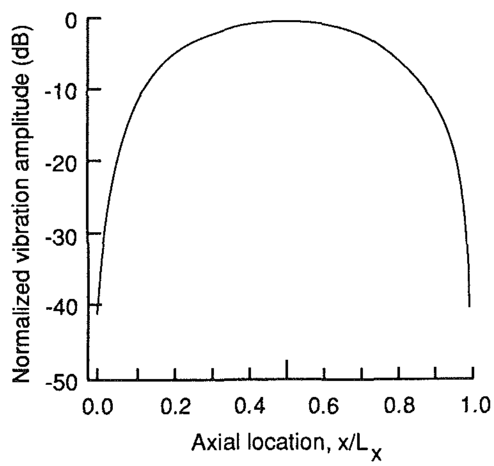

Fig. 8 Displacement distribution, configuration II, $\omega = 930$ rad/sec

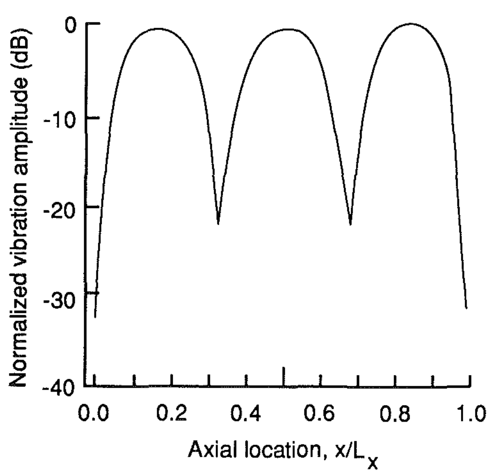

Fig. 7 Displacement distribution, configuration I, $\omega = 1700$ rad/sec

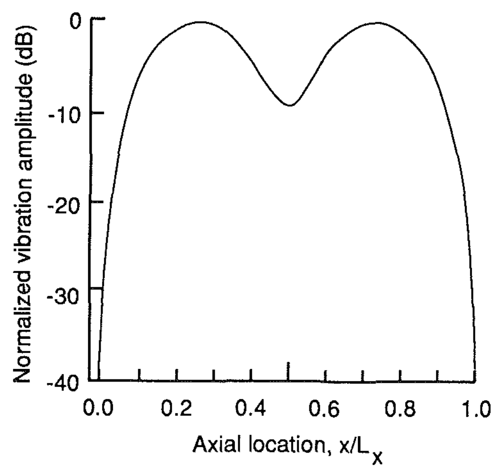

Fig. 9 Displacement distribution, configuration III, $\omega = 600$ rad/sec

Table 5 Plate displacement amplitudes (dB), $\omega = 600$ rad/sec)

m \ n	1	2	3	4	5	6
1	- 2.27	-625.1	-37.2	-642.6	-46.4	-640.7
2	0.0	-623.9	-33.5	-638.2	-41.6	-635.7
3	- 6.5	-625.4	-33.2	-637.1	-40.1	-633.9
4	-10.8	-628.1	-34.7	-637.8	-40.4	-633.9
5	-14.5	-631.1	-37.0	-639.5	-41.7	-634.9
6	-18.8	-634.9	-40.4	-642.5	-44.2	-637.2

Table 6 Plate displacement amplitudes (dB), $\omega = 1700$ rad/sec)

m \ n	1	2	3	4	5	6
1	-39.7	-639.6	-46.3	-654.9	-59.4	-653.9
2	-25.0	-613.4	-44.1	-650.6	-54.6	-648.9
3	0.0	-634.4	-45.1	-649.8	-53.2	-647.1
4	-21.1	-639.7	-47.3	-650.8	-53.6	-647.2
5	-26.8	-643.7	-49.9	-652.7	-54.9	-648.2
6.	-31.7	-647.9	-53.5	-655.7	-57.5	-650.5

Table 7 Plate displacement amplitudes (dB), $\omega = 930$ rad/sec)

m \ n	1	2	3	4	5	6
1	0.0	- 32.8	- 39.1	- 45.7	- 54.9	-343.4
2	-345.8	-348.1	-352.5	-358.5	-367.3	-655.6
3	- 55.4	- 54.3	- 57.2	- 62.4	- 70.8	-358.8
4	-358.5	-356.1	-357.9	-362.3	-370.3	-658.0
5	- 84.7	- 81.6	- 82.6	- 86.5	- 94.1	-381.5
6.	-357.4	-352.2	-355.2	-348.9	-349.1	-350.6

Table 8 Plate displacement amplitudes (dB), $\omega = 600$ rad/sec)

m \ n	1	2	3	4	5	6
1	- 0.8	-599.1	- 4.6	-620.5	-15.2	-617.9
2	-266.4	-808.6	-308.9	-923.8	-318.2	-920.7
3	0.0	-612.1	- 9.7	-623.7	- 17.6	-619.8
4	-310.3	-920.03	-316.2	-929.4	-322.8	-924.7
5	- 11.9	-620.7	- 16.1	-628.6	- 21.6	-623.2
6	-319.4	-927.7	-322.5	-934.6	-327.2	-928.6

little contribution from other modes. The modal amplitudes of Table 4 predict that in this case the (2,1) mode is the dominant mode. Spillover is mainly confined to the other $n=1$ modes, with the strongest excited mode (3,1) being 33 db below the dominant mode. Again, here the $n=2$ nodes cannot couple to the actuator at all, while there will be some coupling to the $n=3$ nodes.

Excitation Frequency $\omega = 600$ rad/sec. This excitation frequency was chosen as it is between the resonances of (1,1) and (2,1) and the system is being driven off-resonance or "forced" into motion. The displacement distribution in this case, Fig.6, shows evidence of multi-modal excitation and this is confirmed in the modal amplitudes of Table 5. At this frequency for this shape of actuator, weak dominance occurs in the (2,1) and (1,1) modes. However, strong spillover occurs in the other $n=1$ modes. It is also apparent from Fig. 6 that for this case there is a strong node being forced close to the $x=x_1$ actuator boundary. Reasons for this will be discussed later. It is also clear that for this location and size of the actuator, modes that will be excited are those whose shape has in-phase portions at the $y=y_1$ and $y=y_2$ actuator boundaries.

Excitation Frequency $\omega=1700$ rad/sec. Here the excitation frequency is close to the (3,1) mode resonance. Figure 7 and Table 6 show a clear dominance of the (3,1) mode with relatively little spillover to lower and higher modes.

Variation of the Actuator Location. In this case the actuator was rotated to be long in the x-direction and narrow in the y-direction. Its location was changed to $x_1=0.04$ m, $x_2=0.34$ m, $y_1=0.23$ m and $y_2=0.27$ m corresponding to configuration II. Thus, the actuator is symmetric about the $x=L_x/2$ line. The excitation frequencies were the same as in the previous cases.

Figure 8 is representative of the results for this configuration. The excitation frequency is very close to the (2,1) mode resonance but the vibration profile shows no trace of that mode shape. Instead the (1,1) mode seems to dominate. Table 7 gives the relative modal amplitudes. It is seen that it is both the (1,1) and the (1,3) modes that dominate and spillover mainly occurs into modes with nodal lines parallel to the x axis.

When the excitation frequency was close to the (1,1) or the (2,1) mode resonance it was observed that it was possible to excite only the (1,1) mode with this configuration actuator. The same was observed when the actuator was driven at frequencies between the first two resonances.

Spillover is observed mostly to the higher modes (3,1), (1,3), (3,3), etc. The location of the actuator in relation to the excited mode shapes is such that the actuator boundaries are always at in-phase areas of these mode shapes. The inability of this actuator to excite the (2,1) mode becomes, therefore, clear since the actuator boundaries $y=y_1$ and $y=y_2$ are located at out-of-phase regions of this mode shape. As the effective edge moments attempt to excite the (2,1) mode, they act against each other because of their in-phase action. In the excited mode, however, the in-phase actuator boundary moments cooperate with each other, since they act upon in-phase regions of the corresponding mode. Thus in Fig. 8 it is obvious that the $x=x_1$ and $x=x_2$ boundary moments excite the (1,3) mode.

Small Actuator at the Plate Center. A small actuator was next considered located at the center of the plate: $x_1=0.16$ m, $x_2=0.22$ m, $y_1=0.13$ m, $y_2=0.17$ m corresponding to configuration III. The same four excitation frequencies were examined.

It was by now expected that the (1,1) mode would be strongly excited when driven near its resonance. The vibration profile was similar to that resulting from the other actuator locations and will not be presented here. As far as the (2,1) mode excitation is concerned, the actuator is located symmetrically across the (2,1) nodal line at $L_x/2$. The results obtained prove that it is impossible to excite that mode when the plate is driven near its resonance frequency and most of the response again occurs in the (1,1) mode. When the plate is driven off-resonance at $\omega=600$ rad/sec with this shape of actuator wide spread spillover occurs into the symmetric modes ($m=1,3,5,\ldots$; $n=1,3,5,\ldots$) while the asymmetric modes ($m=2,4,6,\ldots$; $n=2,4,6,\ldots$) are not excited at all. It can be easily seen that for all modes excited in this case, the whole actuator is located within a single antinodal region; hence it is relatively well coupled to all these modes.

Table 8 gives the relative modal amplitudes for the $\omega=600$ rad/sec case showing these features and Fig. 9 depicts the vibration profile for this excitation. The multimodal characteristic of the response is clearly evident. Notice that the actuator is effectively trying to force a nodal line at the center of the plate, that is close to its boundaries. It is suspected that actually the actuator tries to force two nodes close to its $x=x_1$ and $x=x_2$ boundaries. The proximity of these lines, however, result in what is apparently a (2,1) modal displacement pattern although that mode is not excited at all. What is seen in Fig. 9, instead, is the superposition displacement response of the many excited modes, which tend to cancel each other near the actuator edge.

Concluding Discussion

A theory for the excitation of two-dimensional thin elastic structures by patch type piezoelectric actuators bonded to the structure surface has been developed. This theory has been briefly applied to excitation of a simply supported rectangular thin plate by a single rectangular actuator consisting of two piezoelectric actuators bonded symmetrically to both sides of the plate.

Although the initial study is brief, a number of important results are immediately apparent.

(*1*) From the results of the analysis it appears possible to excite modes in two dimensional structures using patch type actuators.

(*2*) The input frequency of the excitation markedly affects the modal responses. When close to the resonant frequency of a mode, that mode is dominantly excited provided the actuator is properly located. Off resonance, the modal distribution is dependent upon patch shape and location.

(*3*) The location of the actuator strongly influences the ability of the actuator to excite certain modes as well as the spillover. Since all the edges of the actuator act in phase, parallel edges may cooperate or cancel each other as far as the excitation of a particular mode is concerned. When a mode is such that parallel actuator edges are located in regions of the plate having 180 deg phase difference, then these actuator edges cannot couple well to that mode. If these parallel edges are in addition symmetrically positioned about the nodal line that separates those out-of-phase regions, coupling becomes theoretically impossible.

Spillover will in general occur among modes that can couple to the actuator according to the above observations. This is evident in all the tables containing relative modal amplitudes.

(*4*) There is also some evidence from Fig. 6 and Fig. 9 that the actuator tends to force nodal lines in the plate displacement near its boundaries, in the off-resonance case when the response modal density increases. Of course at a node, although the displacement is zero, there is still an effective moment about a nodal line. Since here a nodal line tends to be forced near an actuator boundary, it may be implied that the optimum boundaries of the actuator are along nodal lines or at clamped edges when selected modes are to be excited.

Thus the results show that two dimensional patch type actuators show large potential for controlling vibration in distributed systems. Being distributed in nature it appears possible to tailor the shape of actuator to selectively excite certain modes and suppress others whose response will cause a reduction in performance of controllers, etc., as contrasted to point force actuators which are "spectrally white." As the piezoelements act by exerting a moment they can also be located near nodal lines or the boundaries of plates where the input mobility to point force excitation is low.

Future work will concentrate upon studies of the behavior and derivation of the configuration of optimally shaped actuators as well as configurations for control with single or multi-actuators, independently controlled.

Acknowledgment

The authors gratefully acknowledge the support of the Office of Naval Research under grant ONR N00014-88-K-0721.

References

1 Meirovitch, L., and Norris, M. A., 1984, "Vibration Control," *Proceedings of Inter-Noise 84*, pp. 477-482.

2 Fabunni, J. A., 1980, "Forced Vibration of a Single-Stage Axial Compressor Rotor," ASME *Journal of Engineering Power*, Vol. 120, No. 2, pp. 322-328.

3 Swigert, C. J., and Forward, R. L., 1981, "Electronic Damping of Orthogonal Bending Modes in a Cylindrical Mast—Part I: Theory, Part II: Experiment," *Journal of Spacecraft and Rockets*, Vol. 18, No. 1, pp. 5-17.

4 Hanagud, S., Obal, M. W., and Meyyappa, M., 1985, "Electronic Damping Techniques and Active Vibration Control," *AIAA Paper* 85-0725.

5 Crawley, E. F., and de Luis, J., 1987, "Use of Piezoelectric Actuators as Elements of Intelligent Structures," *AIAA Journal*, Vol. 25, No. 10, pp. 1373-1385.

6 Bailey, T., and Hubbard, J. E., 1985, "Distributed Piezoelectric-Polymer Active Vibration Control of a Cantilever Beam," *AIAA Journal of Guidance and Control*, Vol. 6, No. 5, pp. 605-611.

7 Fanson, J. L., and Chen, J. C., 1986, "Structural Control by the Use of Piezoelectric Active Members," *Proceedings of NASA/DOD Control-Structures Interaction Conference*, NASA CP-2447, Part II.

8 Baz, A., and Poh, S., 1987, "Optimum Vibration Control of Flexible Beams by Piezoelectric Actuators," NASA CR-180209.

9 Timoshenko, S., and Woinowsky-Krieger, 1959, *Theory of Plates and Shells*, McGraw-Hill, NY.

10 Liang, C., and Rogers, C. A., 1989, "Behavior of Shape Memory Alloy Actuators Embedded in Composites," *Proceedings of the 1989 International Composites Conference*, Beijing, China, August.

11 Morse, P. M., and Ingard, K. V., 1968, *Theoretical Acoustics*, McGraw-Hill, NY.